Towards Risk and Resilience Quantification of Gas Networks based on Numerical Simulation and Statistical Event Assessment

Sebastian Ganter[1], Kushal Srivastava[1], Georg Vogelbacher[1], Jörg Finger[1], Bogdan Vamanu[2], Vytis Kopustinskas[2], Ivo Häring[1] and Alexander Stolz[1]

[1]*Safety Technology and Protective Structures Department, Fraunhofer Institute for High-Speed Dynamics, Am Klingelberg 1, 79588 Efringen-Kirchen, Germany.*
E-mail: Sebastian.Ganter@emi.fraunhofer.de

[2]*Directorate for Energy, Transport and Climate, Joint Research Centre (JRC), European Commission, E. Fermi 2749, 21027, Ispra (VA), Italy*

Natural Gas consumed in Europe is mainly imported via pipelines from Russia, Norway and Algeria. Disruption to the gas network can have serious impact on the supply of gas to the consumers within the gas network and therefore should be prevented. In order to make the European gas network more resilient to disruptions due to various causes predictive network simulations and subsequent statistical evaluation procedures are being used to generate a capability to identify the most vulnerable and most important parts of the network. The current work outlines the implementation of a zero-dimensional steady state gas network simulation code applying the momentum and mass conservation equation. The resulting non-linear system of equations is solved with a standard solver based on the Newton approach. As a result, pressure at the consumer ends are calculated for all disruption scenarios that include one single disrupted pipeline. Based on these calculated pressures a statistical evaluation of the importance of pipelines and the vulnerability of nodes is carried out. This approach is demonstrated using a small model of the Irish natural gas network including 14 pipelines and 13 nodes.

Keywords: Resilience Assessment, Gas Network Simulation, Gas Flow Equations, Statistical Analysis, Critical Infrastructure, Safety and Security.

1. Introduction

1.1. *Motivation*

Natural gas is one of the most important energy sources. The world's primary energy consumption in 2018 was covered with a share of about 22.9 % by natural gas and will even increase to about 25 % in 2040, see e.g. International Energy Agency (2019). Natural gas is also an essential part of the energy supply in the European Union (EU). It is mainly used to generate electricity, to heat commercial and private households, as a heat source and raw material in thermal industrial processes and as a fuel in the transport sector. Natural gas consumed in Europe is mainly imported via pipelines from Russia, Norway and Algeria. In terms of the past five years, domestic natural gas production in the EU has been declining which results in an increasing dependency on imports (The European Commission EUROSTAT (2019)). The gas is imported, transported and distributed within Europe by a gas network of 140 000 km (European Gas Pipeline Incident Data Group (2018)) including pipelines, compressor stations, gas storages and other components. Thereby the gas network represents an extremely sensitive infrastructure, the security of which must be constantly improved.

Potential risks that may compromise the security of gas supply are e.g. accidental and intentional external interference, corrosion, construction defects, material failure and ground movement as well as geo-political or societal-political unrest that can lead to disruptions. These, in turn, can have serious impacts on the supply of gas to the consumers within the gas network and therefore, should be prevented.

As a result of the January 2009 dispute between Russia and Ukraine that caused major supply disruption in some parts of Europe, the European Commission (EC) adopted Regulation 994/2010 (Council of European Union (2010)) on security of gas supply, which asks the EU Member States to fulfill a number of requirements. These requirements include risk assessment, preventive action and emergency action planning, installation of cross border reverse flow capabilities and supply and infrastructure standards based on the N-1 criterion[a]. In addition, in 2017 the new Reg-

[a]The N-1 criterion shows how sustainable the gas network is when the single largest element is disrupted.

Proceedings of the 30th European Safety and Reliability Conference and the 15th Probabilistic Safety Assessment and Management Conference
Edited by Piero Baraldi, Francesco Di Maio and Enrico Zio
Published by Research Publishing, Singapore.
ISBN: 978-981-14-8593-0; doi:10.3850/978-981-14-8593-0

ulation 2017/1938 (Council of European Union (2017)) came into force introducing also a solidarity mechanism among the countries in case of gas supply emergencies.

This work is a part of an EU project (SecureGas CORDIS (2019)) funded under Horizon 2020 to enhance and ensure resilience of supply of natural gas within EU states. Under this project, in order to make the European gas network more resilient to disruptions due to various causes predictive network simulations and subsequent statistical evaluation procedures are being used to generate a capability to identify the most vulnerable and most important parts of the network.

1.2. *State of the art and general procedure*

Risk assessments and other analysis in the context of gas supply networks are often based on the evaluation of gas supply scenarios. This essentially requires the prediction of the gas flow rates within the gas network for various disruption scenarios which are needed to be calculated beforehand. Therefore, the network needs to be described using a reasonable level of detail. Commonly it is composed of several elements like pipelines, gas source, gas consumers, junctions, storages and compressors. The general procedure can then be depicted within three steps:

- Starting from the undisturbed network topology one or more elements of the network are considered as disrupted. This means that either the element is completely disabled or is working at partial capacity. In the case of a pipeline disruption e.g. it is assumed that the pipeline cannot be used for gas transmission any more since it has to be shut-off by valves.
- Based on such a scenario the gas flow is numerically predicted whereby several approaches can be used as detailed in the subsequent subsection.
- Repeating such calculations for many possible disruption scenarios then provides the base for statistical analysis of the security of supply and other risk related quantities.

As one of the approaches recently used to predict gas flow within the network is the Maximum Flow algorithm. It predicts the hypothetical maximum gas flow based on predefined pipeline capacities restricting the flow for each single pipeline. This approach was used in Praks et al. (2015) and Kopustinskas et al. (2018) using the Ford-Fulkerson algorithm for the maximum flow (max-flow) calculation. For risk assessment purposes, the max-flow approach was applied for disruption scenarios generated using the Monte-Carlo method based on failure-rates for all elements of the network. These results were then evaluated statistically.

One of the limitations of the max-flow approach is that it does not account for the physical behavior of gas flows. In turn, it cannot compute the gas pressure at the consumer ends. However, since gas consumers require certain minimum pressures to operate, the max-flow algorithm might predict a sufficient gas supply overseeing the fact that the gas cannot actually be used. To address this problem, in the present work a steady-state flow equation solver is implemented that provides the needed pressure information across the entire network. Furthermore, a supply assessment based on a deterministic approach is used. Hereby, all one-pipeline-disruption scenarios (singe pipeline loss) are calculated to obtain a database on which two basic risk related evaluation approaches are applied.

1.3. *Structure of the current work*

After this introduction, section 2 describes how the gas network is captured within this work and how the mathematical problem is formulated. This includes the introduction of the physical equations that need to be solved and also the type of boundary conditions that are needed to get the flow rates and pressures within the gas network. After a basic verification depicted in section 3, the application of the newly implemented solver is described in section 4. It provides the general procedure, the results and also corresponding statistical evaluations. The last section (section 5) concludes with a summary and an outlook.

2. Governing Equations and Problem Formulation

With the overarching goal of supply assessment of the gas at the consumer ends, it is advisable to calculate pressures and mass flows within the gas network. Furthermore, we are interested in the equilibrium state, i.e. the state that is theoretically reached after infinitely long time. A necessary criterion for the existence of a steady-state in general is that the boundary conditions of the considered system do not change over time. This is the case assuming that immediate measures such as shutting off the affected pipeline are very quick on the one hand and repairing the pipeline on the other is very slow. So that the period in between, which is considered in the simulation, is long enough to reach a new steady state.

With pressure and mass flux there are two variables that have to be solved for. This requires solving two equations that relate these quantities. Therefore, the momentum and the mass conservation equations as given by Eq. (1) and (2) are solved. Since the mass conservation includes the density as a third unknown variable, a third equation, the equation of state according to Eq. (3), has to be added in order to obtain a solvable system

of equations. With this and also in accordance with Ekhtiari et al. (2019), the following set of equations need to be solved, where Eq. (3) has already been taken into account in Eq. (1).

$$\frac{\partial p}{\partial x} = -\frac{f \rho_n^2 Z R T Q |Q|}{\eta_t^2 D A^2 p} - \frac{g \sin(\theta)}{ZRT} p \quad (1)$$

$$\frac{\partial (\rho w)}{\partial x} = 0 \quad (2)$$

$$\frac{p}{\rho} = ZRT \quad (3)$$

Hereby p represents the pressure, f the friction factor, Z the compressibility factor, R_s the specific gas constant, T the temperature, Q the (normalized) flow rate, D the pipe diameter, A the cross-section area, ρ the density, ρ_n the density at standard conditions, w the mean velocity of the gas, g the gravitational acceleration and θ the inclination of the pipeline relative to the horizontal line.

At this point, it is important to point out the relationship between the mass flux and the (normalized) flow rate: The flow rate Q which denotes a volume flux having the unit standard cubic meters per second is actually defined by the mass flux:

$$\dot{m} = \rho_n \cdot Q \quad (4)$$

and is therefore not dependent on pressure or temperature. In this work the unit $(\mathrm{sm}^3/\mathrm{s})$ is used whereby the first s refers to *standard*. The friction forces due to the no-slip boundary condition at the pipe walls, which also would lead to gradients in radial direction, are captured using the Darcy-Weisbach-equation Brown (2000) represented by the first term of Eq. (1) on the right-hand side. The second term accounts for the inclination of the pipeline. The compressibility Z, that occurs in Eq. (3), can be calculated as described in Heidaryan et al. (2010). Furthermore, within this work the temperature is assumed to be constant at 288.15 K, since pipelines mostly take on the ambient temperature and the considered scenarios neither include gas compressor stations nor pressure reducers.

As the pipelines are considered to have a constant diameter and flow rate along their longitudinal axis, Eq. (1) and (2) can be integrated along this coordinate turning the set of differential equations into a set of algebraic equations. Setting up one momentum equation for each pipe and one mass conservation equation for each node a non-linear equation system is obtained (see e.g. Ekhtiari et al. (2019)), which can be solved by standard solvers. For the present work this is done using the Newton-Krylov method (Knoll and Keyes (2004)), which is available in PYTHON standard libraries.

To obtain an equation system that can be solved properly, some constrains regarding boundary conditions need to be fulfilled. Beside others, this includes the requirement to include at least one pressure boundary condition as well as at least one mass flow boundary condition anywhere in the gas network. Violation of this rule would result in an ill-conditioned equation system, that would, in turn, prevent the solver from convergence. As an initial solution to start the solver, a vanishing flow rate for all pipes and pressure equal to the supply pressure for all nodes is chosen.

3. Basic Verification

In order to test and verify the implementation of the steady-state gas network solver that is implemented as part of this work, two simple test-cases are considered. The first one described in section 3.1 focuses on the prediction of pressure loss due to the friction term. The second test-case, on the other hand, focuses on mass conservation within junctions (section 3.2). Both test-cases are kept simple such that an analytical solution is available which is then used to compare the simulation results.

3.1. *Three-nodes-in-a-row test-case*

The first verification test-case includes three nodes and two pipelines as can be seen from Figure 1: Node (1) is considered as a gas source at a

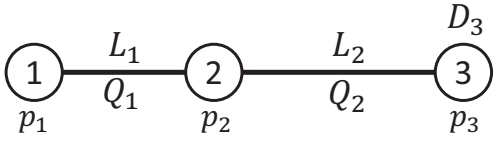

Figure 1. Three-Nodes-in-a-Row Test-Case

constant pressure of $p_1 = 70\,\mathrm{bar}$. Node (3) is defined as a consumer with a gas demand of $D_3 = 10\,\mathrm{sm}^3/\mathrm{s}$. Pipeline (1) and (2) are defined to have a length of $L_1 = 100\,\mathrm{km}$ and $L_2 = 200\,\mathrm{km}$, respectively. Furthermore, a diameter for each is set to 0.7 m, the friction factor is set to 0.01, the density at standard conditions ρ_n is assumed to be $0.668\,\mathrm{kg}/\mathrm{m}^3$ and the product ZRT is set to $128886.6\,\mathrm{J}/\mathrm{kg}$. Finally, the nodes are assumed to have the same height. By this, the test-case is fully defined such that the implementation returns the results presented in Table 1. As can be seen from the table, the flow rate in both pipelines equals the demand of the consumer, which is consistent with the mass conservation equation (Eq. (2)). Furthermore, the pressure in node (2) and (3) can be verified by integrating Eq. (1) along the pipeline length resulting in the algebraic expression for

Table 1. Simulation results for three-nodes-in-a-row test-case.

j (-)	Pressure at node j (bar)	i (-)	Flow rate in pipeline i (sm^3/s)
1	70.000	1	10.0
2	69.960	2	10.0
3	69.881		

pipeline (1) and (2), respectively:

$$p_1^2 - p_2^2 \stackrel{?}{=} 16 f \rho_n^2 Z R T L_1 \pi^{-2} D^{-5} |Q_1| Q_1 \quad (5)$$
$$\mathbf{55474153}098.8 \approx \mathbf{55474153}769.8$$
$$p_2^2 - p_3^2 \stackrel{?}{=} 16 f \rho_n^2 Z R T L_2 \pi^{-2} D^{-5} |Q_2| Q_2 \quad (6)$$
$$\mathbf{11094830}8268.7 \approx \mathbf{11094830}7539.5$$

Evaluation of Eq. (5) and Eq. (6) reveals that the results satisfy the equations for the first eight digits. Hence the relative error is on the order of 10^{-8}.

3.2. *Junction test-case*

The second verification test-case includes four nodes and three pipelines as can be seen from Figure 2. This test-case mainly focuses on checking

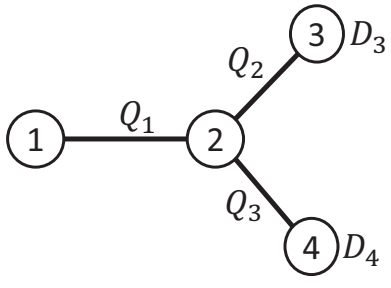

Figure 2. Junction Test-Case

the mass conservation at the junction node (2). Once more, node (1) is considered as a gas source and node (3) and (4) are considered as consumers demanding $10\,\mathrm{sm}^3/\mathrm{s}$ and $20\,\mathrm{sm}^3/\mathrm{s}$, respectively. Using the diameters, friction coefficients, density and the product ZRT given in the first test-case, the simulation returns the flow rate results given in Table 2. As Q_3 equals D_4, Q_2 equals D_3 and Q_1 equals the sum of Q_2 and Q_3, the mass conservation equation is fulfilled accurately. By this result a basic verification of the newly implemented gas network solver is conducted successfully. However, further verification test-cases including larger networks are planned for subsequent works.

Table 2. Simulation results for the junction test-case.

j (-)	Pressure at node j (bar)	i (-)	Flow rate in pipeline i (sm^3/s)
1	70.000	1	30.0
2	69.642	2	10.0
3	69.603	3	20.0
4	69.483		

4. Application

The simulation approach is applied to an abstract, simplified model of the Irish natural gas network. In the subsequent sections the gas network topology together with its boundary conditions that are taken from Ekhtiari et al. (2019) is described.

4.1. *Gas network topology*

The considered gas network includes $N = 13$ nodes and $M = 14$ pipelines. Three of the nodes are defined as gas sources ($j = 1, 2, 3$), the rest are considered as consumers ($j = 4 \ldots 13$) drawing gas out of the system. The topology is given in Figure 3. Furthermore, the pipelines are specified

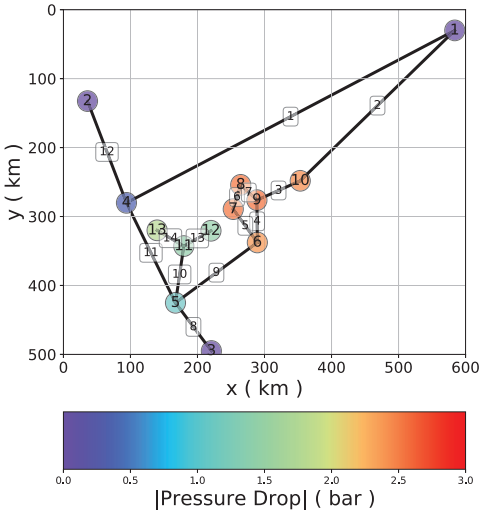

Figure 3. Disruption-free gas network topology with indexing of nodes (circles) and pipes (rectangles) giving the pressure loss in relation to the source pressure.

regarding the nodes they connect to and also their length and diameter as given in Table 3. At this point it should be noted that the pipeline lengths do not correspond to the lengths of the straight connections as shown in Figure 3. Thereby, the

Table 3. Pipeline properties

i (-)	start node (-)	end node (-)	Length L_i (km)	Diameter D_i (m)
1	1	4	550	0.76
2	1	10	200	0.60
3	9	10	50	0.60
4	6	9	15	0.60
5	6	7	20	0.60
6	7	8	18	0.60
7	8	9	8	0.60
8	3	5	25	0.60
9	5	6	70	0.60
10	5	11	65	0.60
11	4	5	150	0.60
12	2	4	135	0.76
13	11	12	15	0.60
14	11	13	13	0.60

Table 4. Boundary conditions for gas supply nodes and consumer nodes, respectively.

j (-)	Type (-)	Pressure (bar)	Demand (sm^3/s)	Height (m)
1	Source	70	-	130
2	Source	70	-	60
3	Source	70	-	60
4	Consumer	-	40	40
5	Consumer	-	30	30
6	Consumer	-	10	60
7	Consumer	-	5	82
8	Consumer	-	5	83
9	Consumer	-	5	85
10	Consumer	-	60	30
11	Consumer	-	10	25
12	Consumer	-	8	30
13	Consumer	-	7	100

length as well as the diameter are included in the friction term of the momentum equation (Eq. (1)) whereas the coordinates of the nodes given in Figure 3 do not enter the calculations.

4.2. *Boundary conditions*

In addition to the topology, boundary conditions have to be set in order to define the physical state of the gas network system. As mentioned in section 2, it has to be defined pressure boundary conditions for the source nodes and demand boundary conditions for the consumers. By this, the assumption is made that sources can provide an unlimited supply of gas mass flux at a constant pressure. In reality, of course, the pressure would drop at some point as the delivery rate is increased. As long as the operating conditions do not differ too much from the design point, however, this assumption is reasonable. On the other hand, at the consumers a constant mass flow is enforced which does not decrease with falling pressure at the consumer. This would primarily occur with significant pressure drops. However, as will be revealed later in the result section (section 4.3.1), the pressure drop at the consumers, that get gas at all, is relatively small. Both types of boundary conditions are given in Table 4 along with the corresponding node type. Furthermore, the table provides the relative height of the nodes which determines the gravity term in the momentum equation (Eq. (1)).

4.3. *Network simulation results*

In order to conduct a vulnerability and an importance analysis several simulations are performed. As a starting point, the described topology is simulated which represents the disruption-free scenario. In a second step all possible one-pipeline-disruption scenarios are simulated and compared with the results of the disruption-free scenario in order to analyze the impact of each pipeline disruption on the pressure of each node separately. Thereby, the number of possible one-pipeline-disruption scenarios equals the number of pipelines such that there are $M = 14$ scenarios.

4.3.1. *Disruption-free scenario*

Using the topology and boundary conditions described in the subsections 4.1 and 4.2, the pressure for each node and the gas flow rate for each pipeline is obtained as given in Table 5. These pressure results will serve as a reference pressure later on in order to assess one-pipeline-disruption scenarios. The left part of the table provides the resulting pressure for each consumer node along with the predetermined pressures at the gas sources ($j = 1, 2, 3$) for orientation. As it can be seen, the pressure drops about 2.5 bar at maximum, so by about 3.5 % of the supply pressure. The right part of the table provides flow rates going through each pipe.

In the case of pipeline $i = 13$ and $i = 14$, the flow rates correspond exactly to the gas consumption of the nodes that are exclusively supplied by these pipelines. For comparison refer Figure 3 and the gas demand given in Table 4 at $j = 12$ and 13.

4.3.2. *One-pipe-disruption scenario*

In the presented work a deterministic vulnerability and importance analysis is provided. Thereby, the analysis is restricted to one pipeline-disruption scenarios. This means that it is assumed that only one pipeline is disrupted at a time. This assumption is typical for this type of study and is reasonable since the probability for n disruptions at the same time scales with the power of n in

Table 5. Pressure and flow rate results for the disruption-free scenario.

j (-)	Pressure at node j (bar)	i (-)	Flow rate in pipeline i (sm^3/s)
1	70	1	24.8717
2	70	2	41.3015
3	70	3	18.6985
4	69.5818	4	19.496
5	68.9312	5	14.2025
6	67.6014	6	9.20247
7	67.4525	7	4.20247
8	67.4339	8	75.4252
9	67.4223	9	43.6985
10	67.5496	10	25
11	68.6032	11	23.2733
12	68.5687	12	38.4016
13	68.2071	13	8
		14	7

case of statistically independent events, e.g. as opposed to coordinated malicious multiple events. Disrupted pipelines are removed from the gas network assuming that no gas escapes the network along the disrupted pipeline. From operational perspective, this would mean shutting off valves in the affected pipeline. The simulation gives the pressure values p_{ij} for each node (index = j), where each disruption scenario is referenced with index = i. A pressure deviation from the disruption-free scenario is calculated using

$$\delta_{ij} = |H\left(p_{0j} - p_{ij}\right)|, \tag{7}$$

where p_{0j} denotes the pressure for node j for the disruption-free scenario. Hereby, the Heaviside step function H is used to ensure that only under-pressure is accounted for. Over-pressure is not seen as problematic as it cannot exceed the source pressure plus the pressure increase due to differences in height. Therefore, over-pressure will not exceed safety limits. By using the Heaviside step function over-pressure is so to speak 'clipped' to the desired pressure such that it does not affect the overall assessment. Finally δ_{ij} is given in Table 6 omitting the source nodes for which the deviation is zero by definition.

4.4. *Vulnerability and importance assessment*

Vulnerability has been defined by Jenelius et al. (2006) as the product of probability of an event and the corresponding exposure. Assuming a constant failure rate per length for all pipelines, the failure probability of a pipeline scales linearly with its length. A multiplication by a failure rate is not carried out, since as a constant it has no influence on the subsequent ranking. Regardless of the

Table 6. Pressure deviations δ_{ij} in bars as defined by Eq. (7).

$i\backslash j$	4	5	6	7	8	9	10	11	12	13
1	0.59	0.22	0.17	0.17	0.17	0.17	0.15	0.22	0.22	0.22
2	0.26	1.17	4.63	4.75	4.84	4.87	6.48	1.18	1.18	1.17
3	0.00	0.00	0.00	0.00	0.00	0.00	3.48	0.00	0.00	0.00
4	0.00	0.00	0.00	0.06	0.17	0.20	0.18	0.00	0.00	0.00
5	0.00	0.00	0.00	0.09	0.07	0.07	0.06	0.00	0.00	0.00
6	0.00	0.00	0.00	0.00	0.04	0.04	0.04	0.00	0.00	0.00
7	0.00	0.00	0.00	0.00	0.00	0.02	0.01	0.00	0.00	0.00
8	1.29	7.33	6.29	6.25	6.23	6.23	6.05	7.38	7.37	7.33
9	0.00	0.00	11.3	11.2	11.2	11.2	10.7	0.00	0.00	0.00
10	0.00	0.00	0.00	0.00	0.00	0.00	0.00	68.6	68.6	68.2
11	0.00	0.74	0.58	0.57	0.57	0.57	0.52	0.75	0.75	0.74
12	1.45	0.75	0.58	0.57	0.57	0.57	0.52	0.75	0.75	0.75
13	0.00	0.00	0.00	0.00	0.00	0.00	0.00	0.00	68.6	0.00
14	0.00	0.00	0.00	0.00	0.00	0.00	0.00	0.00	0.00	68.2

probability of a pipeline disruption, the exposure of a node due to this disruption can be quantified by the pressure deviation at a node compared with the corresponding pressure in the disruption-free scenario (normal operation). Hence, the vulnerability of a consumer node can be calculated by summing up the pressure deviation of each disruption scenario weighted by the length L_i of the disrupted pipeline scaling the probability that it is disrupted.

$$V_j = \sum_{i}^{N} \delta_{ij} \cdot L_i \tag{8}$$

The vulnerability for each node V_j is given in Table 7 revealing node $j = 12$ to be the most vulnerable one. Given a pipeline is disrupted,

Table 7. Vulnerability of the consumer nodes as defined by Eq. (8).

Node index j (-)	Accumulated length-weighted pressure deviation V_j (bar·km)
12	6240
13	6070
11	5213
10	2607
9	2168
8	2164
7	2147
6	2128
5	750
4	605

the importance of this pipeline denotes the impact

of its disruption on all consumers of the network (Jenelius et al. (2006)). Hence, the importance of the pipelines is calculated by summing up the impact in terms of pressure deviations for all consumers according to

$$P_i = \sum_{j}^{M} \delta_{ij}. \tag{9}$$

The importance P_i is given in Table 8, revealing pipeline $i = 10$ to be the most important one. The

Table 8. Importance of the pipelines as defined by Eq. (9).

Pipe index i (-)	Accumulated pressure deviation P_i (bar)
10	205.38
13	68.57
14	68.21
8	61.75
9	55.54
2	30.51
12	7.25
11	5.79
3	3.48
1	2.28
4	0.61
5	0.29
6	0.12
7	0.03

criticality of the pipelines could be calculated by multiplying their importance with their individual failure probabilities which might lead to another ranking result.

4.5. *Analysis of assessment results*

The results of the previous section suggest a closer look at the disruption scenario $i = 10$. Accordingly, Figure 4 presents the corresponding one-pipeline-disruption topology. As can be seen from the figure, the disruption of pipeline $i = 10$ leads to a total loss of supply of node $j = 11, 12$ and 13, that means that the pressure at these nodes becomes zero. This is also visible in Table 6 (row $i = 10$, column $j = 11, 12$ and 13) which reveals a pressure deviation of almost 70 bars. Actually, the pressure of the considered nodes is not obtained in the regular procedure since the nodes were removed from equation system in an automated manner to ensure convergence of the solver. This is also indicated by the white color and the dashed line style of the corresponding circles in the figure.

Since the considered gas network is relatively small only small pressure drops occur due to

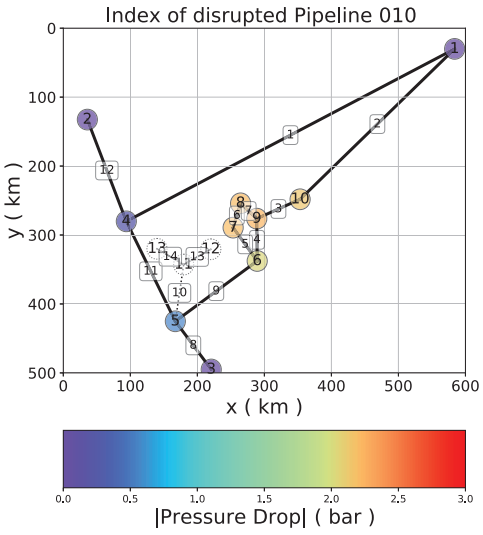

Figure 4. Gas network topology in the case of the disruption of pipeline $i = 10$.

friction within the pipelines. Hence, significant pressure drops only occur if nodes are actually cut off from any supply node. Considering only one-pipeline-disruption scenarios, this is only the case for pipeline $i = 10, 13$ and 14 as can be seen from Figure 4 which leads to the corresponding importance ranking of pipelines given in Table 8. Having a closer look at the most vulnerable nodes ($j = 11, 12, 13$) in Figure 4, it comes clear that these are the only nodes that have only one supplying pipeline connection. For nodes $j = 12$ and 13 this is even more serious since in their case even two disruption scenarios exist, namely $i = 10$ and 13 for the node $j = 12$ and $i = 10$ and 14 for node $j = 13$, that lead to a complete loss of supply. This is clearly reflected by the node ranking in Table 7.

5. Summary and Outlook

The present work described the implementation and verification of a steady-state solver for gas networks consisting of pipelines and nodes predicting flow rates and pressures. Furthermore, the approach was applied to a small example network in order to analyze the impact of disruption of pipelines. Therewith a vulnerability ranking for the consumers nodes and importance ranking for the pipelines could be conducted, whereby the analysis was limited to one-pipeline scenarios. Nodes 11, 12 and 13 could be identified as the most vulnerable ones and pipeline 10 as the most important one, whereby this result could also be obtained by simply looking at the network topology. As mentioned in section 4.3.2 multiple-

pipeline-disruption scenarios are extremely rare. Nevertheless, the investigation is reasonable since their impact is often significantly higher than one-pipeline-disruption scenarios. This is relevant in particular for nodes that are supplied by only a few pipelines, the combined failure of which would mean a complete loss of supply. The challenge hereby is, that the number of possible scenarios O scales with

$$O = \frac{N!}{(N-K)! \cdot K!} = \binom{N}{K}, \qquad (10)$$

where K is the number of disruptions that can occur at the same time and N the number of pipelines within the considered gas network. This relation quickly leads to a number of possible scenarios that can no longer be processed within a reasonable computing time. Going for a more detailed description of the network using for example 100 Pipelines and considering three pipeline-disruption scenarios would already results in $\binom{100}{3} = 161\,700$ scenarios, whereby the computation of each scenario can take several minutes. For this reason stochastic approaches like used in Praks et al. (2015) need to be considered when dealing with large networks, i.e. restricting the analysis to a statistically representative subset of the total set of possible scenarios. Considering multiple-pipeline-disruption scenarios, however, opens the task of optimizing recovery strategies which constitutes a further relevant application of suggested simulation approach.

As it came clear from the result of this work, small networks rather lead to "binary" results. I.e.: Consumers are either (almost) fully supplied or not at all. Within larger networks including longer pipelines the friction at the pipe walls becomes a dominant effect such that the pressure drops become significant along the contribution from other network elements e.g. compressor stations, gas storages and valves. Hence, the entire spectrum between full and not at all supplied can occur at the consumers. Further development will attempt to merge the results of physical simulation with modeling capabilities of the max-flow approach, and therewith enable more reliable vulnerability and importance assessments.

Acknowledgement

This project has received funding from the European Union's Horizon 2020 research and innovation program under grant agreement No 833017.

References

Brown, G. (2000). The darcy–weisbach equation. Website. Online available: http://bae.okstate.edu/faculty-sites/Darcy/DarcyWeisbach/Darcy-WeisbachEq.htm; accessed on 8th of Januar 2020.

CORDIS (2019). Securing The European Gas Network (SecureGas). https://cordis.europa.eu/project/id/833017.

Council of European Union (2010). Regulation (eu) no 994/2010 of the european parliament and of the council. https://eur-lex.europa.eu/eli/reg/2010/994/oj.

Council of European Union (2017). Regulation (eu) 2017/1938 of the european parliament and of the council. https://eur-lex.europa.eu/eli/reg/2017/1938/oj.

Ekhtiari, A. M., I. Dassios, M. Liu, and E. Syron (2019). A novel approach to model a gas network. *Applied Sciences 9*, 26.

European Gas Pipeline Incident Data Group (2018). *Report of the European Gas Pipeline Incident Data Group*.

Heidaryan, E., A. Salarabadi, and J. Moghadasi (2010). A novel correlation approach for prediction of natural gas compressibility factor. *Journal of Natural Gas Chemistry 19*(2), 189 – 192.

International Energy Agency (2019). *World Energy Outlook 2019*.

Jenelius, E., T. Petersen, and L.-G. Mattsson (2006). Importance and exposure in road network vulnerability analysis. *Transportation Research Part A: Policy and Practice 40*(7), 537–560.

Knoll, D. and D. Keyes (2004). Jacobian-free newton–krylov methods: a survey of approaches and applications. *Journal of Computational Physics 193*(2), 357 – 397.

Kopustinskas, V., P. Praks, T. Mara, and R. Rossati (2018). Application of PCE sensitivity analysis method to gas transmission network. In CRC Press (Ed.), *Safety and Reliability – Safe Societies in a Changing World: Proceedings of ESREL 2018*, London, pp. 2693–2700.

Praks, P., V. Kopustinskas, and M. Masera (2015). Probabilistic modelling of security of supply in gas networks and evaluation of new infrastructure. *Reliability Engineering and System Safety 144*, 254 – 264.

The European Commission EUROSTAT (2019). *EU imports of energy products*. The European Commission.